Residual Strength Predictions with Crack Buckling

D. S. Dawicke
NASA LaRC
Hampton, VA 23681, USA
Tel: (757)864-4577
Fax: (757)864-8911
d.s.dawicke@larc.nasa.gov

A. S. Gullerud and
R. H. Dodds, Jr.
University of Illinois
Urbana, Illinois 61801, USA

R. W. Hampton
NASA ARC
Moffett Field, CA 94035, USA

ABSTRACT

Fracture tests were conducted on middle crack tension, M(T), and compact tension, C(T), specimens of varying widths, constructed from 0.063 inch thick sheets of 2024-T3 aluminum alloy. Guide plates were used to restrict out-of-plane displacements in about half of the tests. Analyses using the three-dimensional, elastic-plastic finite element code WARP3D simulated the tests with and without guide plates using a critical CTOA fracture criterion. The experimental results indicate that crack buckling reduced the failure loads by up to 40%. Using a critical CTOA value of 5.5°, the WARP3D analyses predicted the failure loads for the tests with guide plates within ± 10% of the experimentally measured values. For the M(T) tests without guide plates, the WARP3D analyses predicted the failure loads for the 12 and 24 inch tests within 10%, while over predicting the failure loads for the 40 inch wide tests by about 20%.

1. INTRODUCTION

Commercial transport aircraft are designed with a damage tolerant philosophy that permits the aircraft to maintain structural integrity in the presence of long cracks. Continued aircraft safety is obtained through inspections that locate cracks before they reach a size that can lead to the loss of the aircraft. The determination of inspection intervals and locations requires accurate analytical fracture mechanics tools. An important requirement of these analytical tools is the ability to determine the amount of load (residual strength) that a structure can endure for a given crack size. This requires an analytical tool that can predict stable crack growth in a thin ductile material. Additionally, since the fuselage is a pressurized thin-skin structure, crack bulging may be present, detrimentally affecting fracture behavior. An effective analytical tool should provide accurate modeling of crack growth in cases with crack bulging.

Crack bulging is the out-of-plane deformation of the crack faces and surrounding material. In an aircraft fuselage structure, crack bulging results from internal pressure acting in the out-of-plane direction and in-plane compressive stresses along the crack faces. Local crack buckling is likely to occur in thin structures (i.e., if the crack half-length to thickness ratio, a/B, is large) and when the crack face stresses (σ_x) are in compression.

Development of pressure induced crack bulging is difficult in flat laboratory specimens, but local crack buckling occurs naturally in thin, wide specimens. Forman [1] examined the effect of crack buckling on the failure stress of three aluminum alloys and two steels. Identical fracture tests were conducted on flat sheets, with and without guide plates. Figure 1 plots the resulting buckling ratio (the ratio of failure stress without guide plates to failure stress with guide plates) against the ratio of crack length to specimen

thickness. Buckling reduced the failure stress by up to 40%; furthermore, the magnitude of the reduction increased with the ratio of crack half-length to thickness ratio (a/B).

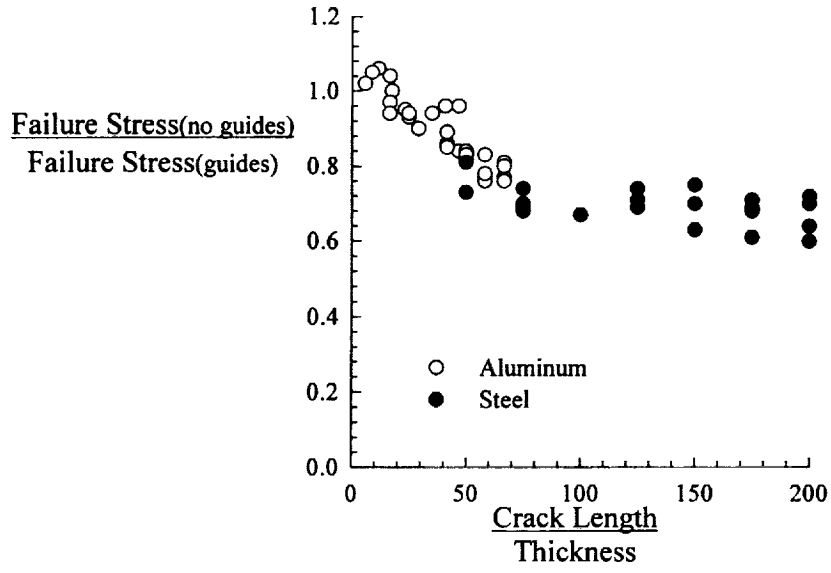

Figure 1. Experimental measurements of the reduction in failure stress due to crack buckling [1].

Finite element predictions of thin aluminum fuselage structures with crack buckling require both an elastic-plastic fracture criterion and a geometrically nonlinear analysis. Thin aluminum structures experience large-scale plastic deformation and extensive stable tearing prior to reaching critical load. Linear elastic fracture mechanics (LEFM) tools do not account for large scale plasticity, thus tend to be structural size dependent [2,3]. Approaches based on elastic-plastic fracture mechanics (EPFM), such as the J-integral resistance curve [4,5], T*-integral resistance curve [6-8], or the critical crack tip opening angle (CTOA) [9-11], are less specimen size dependent [12]. Crack buckling results in local out-of-plane crack displacements that are large relative to the thickness of the material, amplifying crack tip stresses. Modeling the coupling of the membrane stress resultants and out-of-plane displacements requires a geometrically nonlinear analysis [13].

The objective of this paper is to examine the crack tip opening angle (CTOA) fracture criteria, using middle crack tension (M(T)) and compact tension (C(T)) specimens constructed from 0.063 inch thick 2024-T3 aluminum alloy. Fracture experiments using these specimens were conducted with and without guide plates to restrain out-of-plane displacements along the crack face. For cracked thin sheets without guide plates, in-plane compressive stresses along the crack surfaces cause the crack to buckle and exhibit out-of-plane displacements, producing behavior similar to pressure induced crack bulging. To evaluate the effectiveness of the CTOA criterion, analyses using the three-dimensional, elastic-plastic finite element code WARP3D [14] modeled the fracture behavior of the tests. Simulation of the C(T) specimens provided a critical CTOA value that was then used to predict the M(T) tests with and without guide plates. The analyses of the unconstrained (without guide plates) tests employed a geometrically nonlinear formulation to accurately model the large buckling deformations.

2. EXPERIMENTAL PROCEDURE

Fracture tests were conducted on 0.063 inch thick 2024-T3 aluminum alloy M(T) and C(T) specimens. Several different specimen sizes were tested for each of the two specimen types, as summarized in the test matrix shown in Table 1. All of the specimens were precracked at a stress intensity factor range of $\Delta K = 8$ ksi $\sqrt{\text{inch}}$ and a stress ratio of $R = 0.1$. Each specimen was fractured under displacement control at a ramp rate in the range of 0.02 – 0.04 inch/min. Measurements of load, crack extension, crack opening displacement, and out-of-plane displacements were made during the tests. The out-of-plane displacement measurements were performed using a digital image correlation technique [15].

TABLE 1
TEST MATRIX OF THE FRACTURE EXPERIMENTS

C(T)			M(T)		
Width, W (inch)	a/W	Guides	Width, W (inch)	a/W	Guides
2	1/3	yes	3	1/3	no
4	1/3	yes	12	1/3	yes, no
6	1/3	yes	24	1/3	yes, no
			40	1/5	yes, no, p*
			40	1/3	yes, no

* partially constrained, initial guide plates not 100% effective

Guide plates were used to constrain the out-of-plane buckling on some of the M(T) and all of the C(T) specimens. The purpose for the guide plate tests was to decouple the crack growth from the buckling and in the case of the M(T) specimens, to quantify the influence of buckling on the residual strength. The guide plates for the C(T) specimens consisted of two sheets of 1/8 inch thick steel that sandwiched the specimen. Thin strips of Teflon tape were used to reduce friction between specimen and guide plates, while bolts along the edges of the guide plates restricted separation. The guide plates for the M(T) specimens consisted of four sheets of 3/8 inch thick aluminum that formed two "sandwiches" above and below the crack plane, as shown in Figure 2. A pair of 0.5 inch spacer blocks were used to physically separate the top and bottom guide plates, preventing tensile load from being transferred through the guides. This type of guide plate configuration appeared to restrict buckling in specimens as large as 24 inches wide. However, buckling was visible at the center of the crack during the fracture of the 40 inch wide panels. To increase the out-of-plane stiffness of the 40 inch wide guide plates, three sets of 3 inch steel I-beams were placed on both the upper and lower sets of guide plates, as shown in Figure 2.

3. ANALYTICAL PROCEDURE

The elastic-plastic finite element code WARP3D [14] was used to model the fracture behavior of the C(T) and M(T) tests. Simulation of the fracture process employed the crack tip opening angle (CTOA) criterion. This criterion assumes that stable crack extension occurs when the angle made by the upper crack surface, the crack tip, and the lower crack surface reaches a critical value. The measurement of the CTOA on the upper and lower crack surfaces is made at a fixed distance behind the crack tip, taken here to be 0.04 inches [11]. For a buckling crack, where the crack tip region experiences significant deformation, measurement of the CTOA involves tracing an arc along the center of the deformed specimen for a distance of 0.04 inches, then calculating the angle at that location. Linear interpolation between nodes, enables measurement of the CTOA at the correct position. See Figure 3 for a schematic of this process.

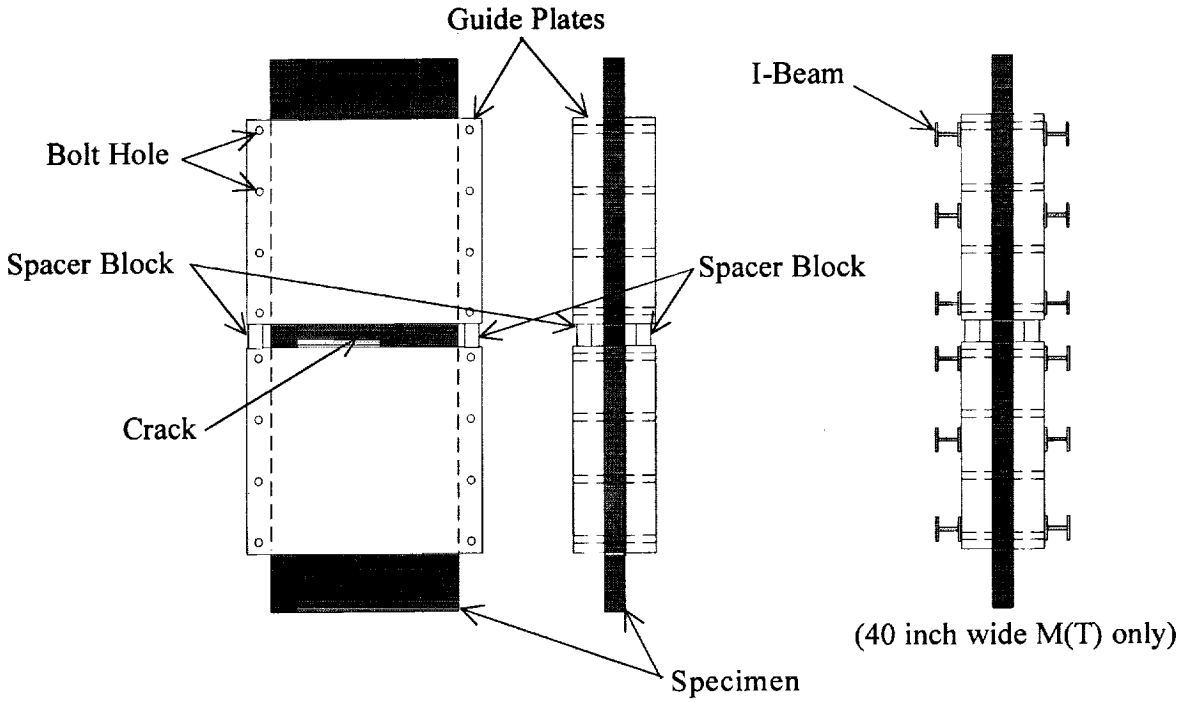

Figure 2. Schematic of M(T) guide plates.

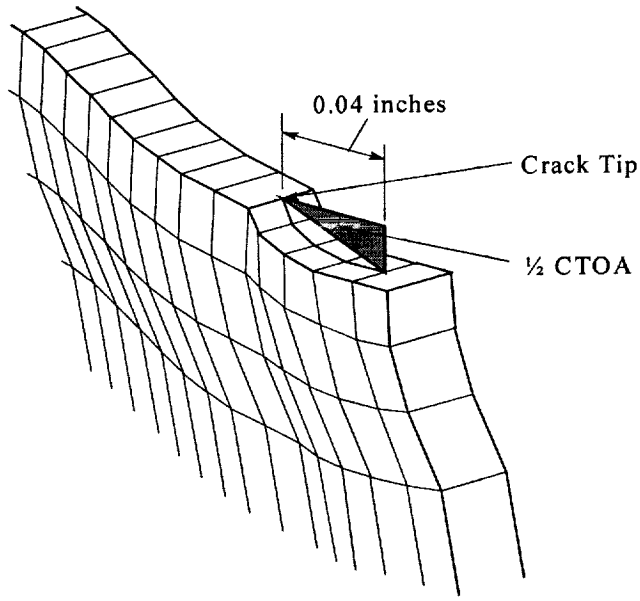

Figure 3 Definition of the critical CTOA for a buckling crack.

To eliminate dependence of the results on mesh resolution, the analyses used multiple elements over the 0.04 inch distance. Simulation of each test used several meshes with increasing refinement, until further refinement produced no significant change in the results; typically, analyses converged using 0.02 or 0.01 inch elements. When the CTOA reached its critical value, all nodes within the 0.04 inch distance released

simultaneously, thereby growing the crack by a 0.04 inch increment. The WARP3D analyses restricted the crack to maintain a straight front through the thickness.

The analyses of the tests with guide plates employed 8-node fully integrated brick elements. The meshes for the unconstrained models primarily utilized 20 node bricks with reduced integration, one element through the thickness. The crack plane, however, consisted of 8-noded elements with four elements through the thickness to support crack growth. Figure 4 shows a typical mesh. Transition elements and rapid geometric transitions served as a bridge between the crack plane elements and the remainder of the mesh. To initiate buckling, the meshes for the unconstrained tests included an initial out-of-plane perturbation, corresponding to either the first buckling mode shape or three-quarters of a cosine wave. The maximum magnitude of the perturbation corresponded to ten percent or less of the specimen thickness. Modal shell analyses conducted in ABAQUS, that utilized the same mesh profile and material description as the WARP3D analyses, provided the buckling mode shapes. Furthermore, the element formulation in WARP3D included the $\overline{B}$ method for alleviating locking in fully integrated elements, as developed by Hughes [17].

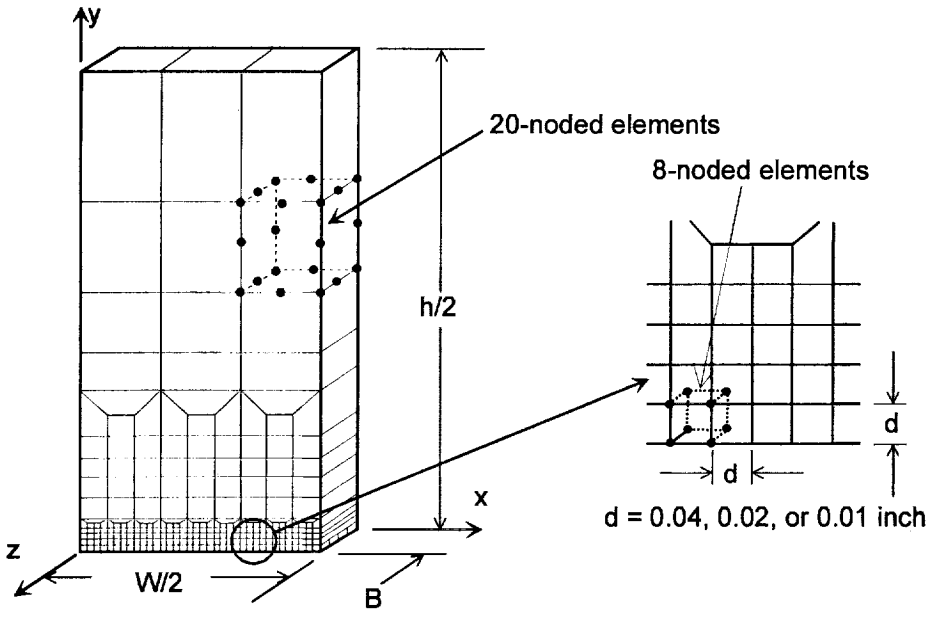

Figure 4. Finite element mesh used to model the 3 inch wide M(T) specimens.

4. RESULTS AND DISCUSSION

The following section contains a summary of all of the experimental fracture results and the WARP3D analyses. The critical CTOA value for the 0.063 inch thick, 2024-T3 aluminum alloy was determined by conducting WARP3D analyses of the C(T) fracture tests. Tables 2 and 3 contains summaries of the test results and analytical predictions for the C(T) and M(T) fracture tests, respectively.

Fracture tests were conducted for 2, 4, and 6 inch wide C(T) specimens. Figure 5 contains the failure load for each of the C(T) tests. At least two identical tests were conducted for each specimen width, producing a maximum difference in failure load of about 6%. Elastic-plastic finite element analyses were

conducted for each test condition using WARP3D. A critical CTOA value of 5.5° provided the best fit for the failure load for all conditions. The maximum difference between the experimental measurements and the WARP3D finite element simulations was 10%. The average difference between the experiments and the predictions, for all of the C(T) tests, was 4%.

TABLE 2
SUMMARY OF EXPERIMENTAL AND PREDICTED FAILURE LOADS FOR THE C(T) FRACTURE TESTS (A/W = 0.4)

Width, W (inch)	Measured Failure Load (kips)	WARP3D	
		Failure Load (kips)	$\frac{P_{prediction}}{P_{test}}$
2	0.71	0.64	0.90
4	1.28	1.20	1.02
6	1.79	1.73	0.97

TABLE 3
SUMMARY OF EXPERIMENTAL AND PREDICTED FAILURE LOADS FOR THE M(T) FRACTURE TESTS

Width (inch)	2a/W	Measured Failure Load (kips)	WARP3D	
			Failure Load (kips)	$\frac{P_{prediction}}{P_{test}}$
3*	1/3	6.85	6.37	0.93
12*	1/3	24.28	23.74	0.98
24*	1/3	43.73	46.27	1.06
40*	1/3	66.78	74.09	1.11
40*	1/5	88.78	92.45	1.04
12**	1/3	20.90	21.24	1.02
24**	1/3	32.21	34.62	1.07
40**	1/3	44.35	53.68	1.21
40**	1/5	60.80	72.37	1.19

* Guide Plates ** No Guide Plates

Fracture tests were conducted on 3, 12, 24, and 40 inch wide M(T) specimens for the 0.063 inch thick 2024-T3 aluminum alloy. The 3 inch wide M(T) specimens were tested without guide plates and no crack buckling was observed. The larger M(T) specimens were tested with and without guide plates and substantial crack buckling was observed for the tests conducted without guide plates.

Elastic-plastic finite element analyses using WARP3D were conducted for each of the specimens tested with guide plates. The critical CTOA value used in the predictions was the same 5.5° obtained from the C(T) analyses. Figure 6 contains the failure stresses for each of the M(T) tests and the corresponding WARP3D analyses. The maximum difference between the experimental measurements and the finite element predictions was 11%. The average difference between the experiments and the predictions, for all of the tests, was 2%. While the average error for all of the WARP3D predictions looks excellent, the analyses increasingly over-predict the failure stress for larger specimen widths. This trend has three possible explanations: (1) the finite element model of the larger specimens may be too stiff, (2) the critical CTOA may be a mild function of specimen width, or (3) the guide plates may not have completely eliminated crack buckling.

To investigate the stiffness of the finite element models, select analyses were duplicated using different mesh resolutions to conduct convergence studies. The convergence studies explored reducing the element size along the crack plane (keeping the distance for measuring the CTOA constant), increasing the number of element layers through the thickness, and increasing the volume, around the crack growth region, modeled with the smallest size elements. These analyses confirmed that the meshes in this study produced converged results. Furthermore, the $\overline{B}$ formulation in WARP3D alleviates the effect of element locking; therefore, neither mesh resolution nor locking appear to have influenced the stiffness of the finite element meshes.

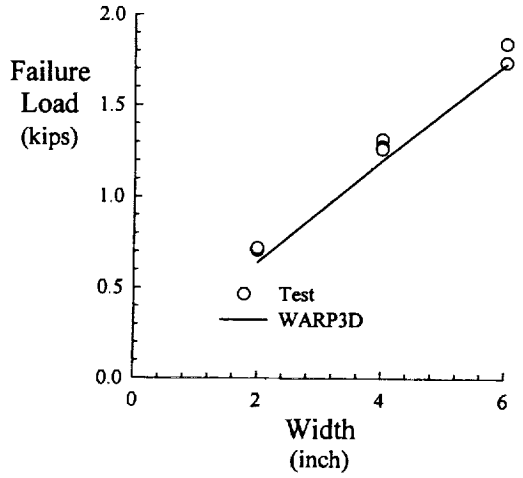

Figure 5. Measurements of failure load against specimen width for C(T) fracture tests (a/W=0.4) and the WARP3D finite element simulations with a critical CTOA of 5.5°.

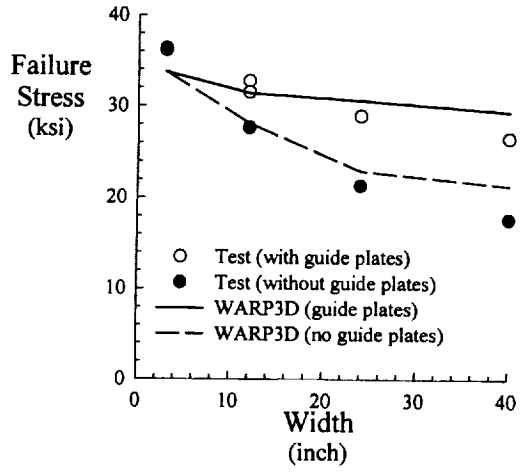

Figure 6 Measurements of failure stress against specimen width for M(T) fracture tests (2a/W=1/3) and the WARP finite element simulations with a critical CTOA of 5.5°.

The critical CTOA value of 5.5° results in an almost exact prediction of the behavior of the 12 inch wide M(T) fracture tests using WARP3D. The critical CTOA values required to "exactly" match the 24 and 40 inch wide M(T) fracture tests would be about 5.3° and 5.1°, respectively. This indicates that the CTOA fracture criterion is at worst, a mild function of specimen width.

The use of guide plates was intended to decouple the crack growth from the buckling behavior, allowing geometrically linear analyses to effectively model the crack growth. The guide plates shown in Figure 2 were sufficient to prevent buckling in the 12 inch and 24 inch wide panels, but the guide plates alone did not prevent buckling in the 40 inch wide panel. The initial 40 inch wide guide plates consisted of four 3/8 inch thick sheets of aluminum that sandwiched the specimen. Teflon sheets were placed between the guide plates and the specimen to reduce the friction between the specimen and guides. The 40 inch wide M(T) specimen tested with the guide plates experienced a 24% increase in failure stress over the unconstrained test, as shown in Figure 7. However, the guide plates were observed to deform out-of-plane about 0.1 inches, indicating that the stiffness of the guide plates was not sufficient to prevent buckling. The out-of-plane stiffness of the guide plates was increased by attaching six pairs of I-beams to the outside of the plates, as shown in Figure 2. A third, identical specimen was tested with the modified guide plate configuration and the measured failure stress was 46% larger than the unconstrained test, as shown in Figure 7.

The unconstrained, partially constrained, and I-beam constrained tests illustrate the difficulty in obtaining completely constrained conditions for wide, thin panels and the strong influence of even a small amount of crack buckling on residual strength. The guide plates that partially constrained the specimen greatly restricted the out-of-plane displacements (from about 1.0 inch in the unconstrained test to about 0.1 inches in the partially constrained test), yet the failure load was 18% lower than the test with the more effective guide plates. It is possible that the I-beam guide plates did not entirely restrict the buckling effects on the fracture behavior, indicating a lower failure stress than would be present in a completely constrained test.

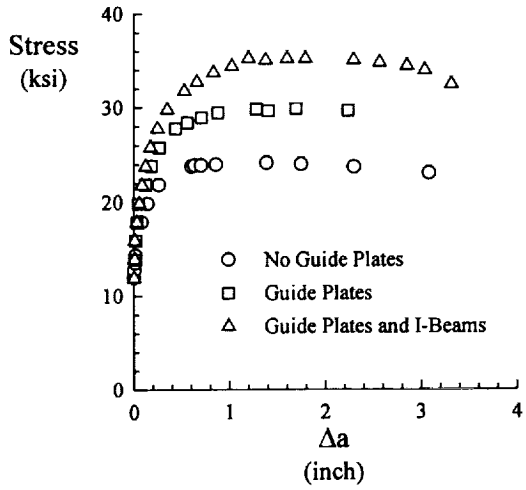

Figure 7. Measurements of stress against crack extension for the 40 inch wide M(T) test with an initial crack length to width ratio of 2a/W = 0.2.

The fracture tests conducted without guide plates experienced significant out-of-plane displacements and exhibited reductions in residual strength of up to 40% compared to identical constrained tests. In all tests, both the upper and lower crack surfaces buckled in the same direction. Reference 15 provides details on out-of-plane displacement measurements made for these tests. Figure 8 plots out-of-plane displacement measurements against the distance from the center of the specimen for 12 inch, 24 inch, and 40 inch wide M(T) fracture tests. The out-of-plane displacement measurements were made 0.5 inches above the crack plane, for a load condition near the failure load of each test. The maximum displacement at the center of the specimen was about 1.0, 0.5, and 0.25 inches for the 40, 24, and 12 inch wide M(T) specimens, respectively. To illustrate the differences in the shapes of the curves, the out-of-plane displacement (w) for each specimen was normalized by the maximum displacement (w_{max}), while the distance from the center of the specimen (x) was normalized by the half width of the specimen (W/2), as shown in Figure 9. The normalized displacements indicate that the 24 and 40 inch wide specimens exhibit considerable secondary buckling at about 2x/W = 0.5 and -0.5. The secondary buckling was almost nonexistent in the 12 inch wide specimen.

Geometrically nonlinear, elastic-plastic finite element analyses using WARP3D were performed for each of the tests conducted without guide plates; Figure 6 displays the results. The critical CTOA value used in the predictions was the same 5.5° used in the other analyses. The WARP3D analyses predicted within 7% the fracture behavior of the 12 inch and 24 inch wide specimens with crack buckling, but over-predicted the failure stress of the 40 inch wide specimen by 21%. As with the guide plate tests, the analyses over-predict the failure stress for larger specimens. Again, the trend has three possible explanations: (1) the finite element models for the larger specimens may not capture the buckling behavior properly, (2) the critical CTOA may be a mild function of specimen size, or (3) the critical CTOA may be influenced by the large out-of-plane deformations associated with crack buckling. The out-of-plane displacements and secondary buckling of the 40 inch wide M(T) fracture test was much more severe than either the 12 inch or 24 inch wide tests. Additional studies are required to demonstrate that the finite element mesh refinement, sufficient to obtain convergence in the constrained tests, is also sufficient to obtain convergence in the unconstrained tests.

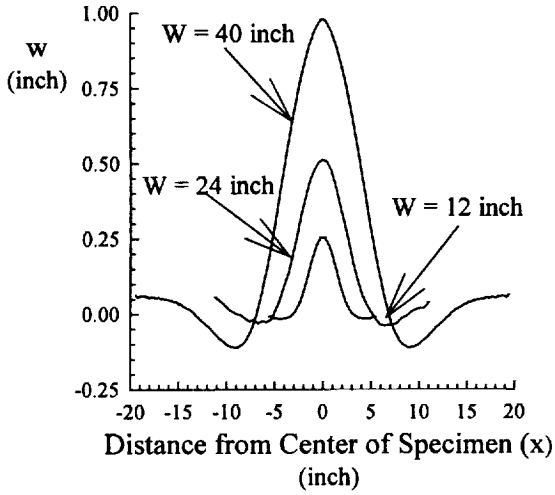

Figure 8. Out-of-plane displacements (w) measured 0.5 inches above the crack plane, at a load near the failure load for three different size M(T) specimens (2a/W = 1/3).

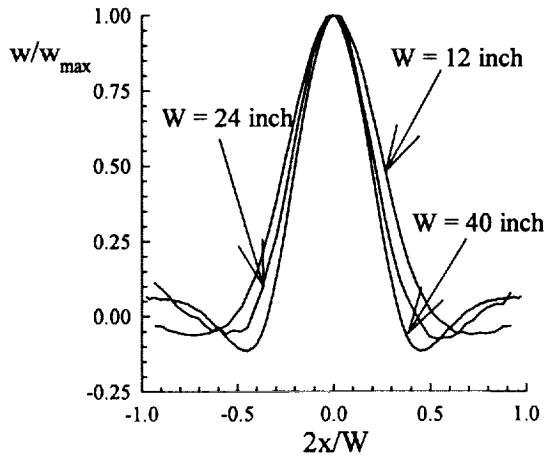

Figure 9. Out-of-plane displacements normalized by the maximum displacement against the distance from the centerline normalized by the half-width for the measurements shown in Figure 8.

5. CONCLUDING REMARKS

Tests were conducted on middle crack tension (M(T)) and compact tension (C(T)) specimens constructed using 0.063 inch thick 2024-T3 aluminum alloy. The C(T) specimens were tested with guide plates to restrict out-of-plane crack buckling, while the M(T) specimens were tested with and without guide plates. The C(T) tests were simulated with WARP3D to determine the critical CTOA value. Using this same CTOA value, the M(T) tests, conducted with and without guide plates, were predicted with WARP3D. The results from this study indicate:

1. Crack face buckling was experimentally shown to reduce the residual strength by as much as 40%.
2. The WARP3D analyses required a critical CTOA value of 5.5° to model the 0.063 inch thick material.
3. The WARP3D analyses predicted the failure load for all of the tests with guide plates to within 10% of the experimental measurements. The average error for all of the tests was small, however, a slight trend in the data indicated that the analyses were increasingly unconservative for larger panels.
4. The WARP3D analyses were able to predict the behavior of the 12 inch and 24 inch wide tests conducted without guide plates within 10%, but overpredicted the behavior of the 40 inch wide test without guide plates by about 20%.

6. REFERENCES

1. Forman, R. G. "Experimental Program to Determine Effect of Crack Buckling and Specimen Dimensions on Fracture Toughness of Thin Sheet Materials", AFFDL-TR-65-146, January 1966.

2. Feddersen, C. E., "Evaluation and Prediction of the Residual Strength of Center Cracked Tension Panels", ASTM STP 486, 1971, pp. 50-79.
3. Wang, D. W., "Plane-Stress Fracture Toughness and Fatigue-Crack Propagation of Aluminum Alloy Wide Panels" Sixth National Symposium on Fracture Mechanics, 1973, p. 334-349.
4. Gudas, J. P. and Davis, D. A., "Evaluation of the Tentative J(I)-R Curve Testing Procedure by Round Robin Tests of HY-130 Steel," Journal of Testing and Evaluation, Vol. 10, No. 6, Nov. 1982, pp. 252-262.
5. Newman, J. C., Jr., Booth, B. C., and Shivakumar, K. N., "An Elastic-Plastic Finite-Element Analysis of the J-Resistance Curve Using a CTOD Criterion," ASTM STP 945, 1988, pp. 665-685.
6. Atluri, S. N., "Energetic Approaches and Path-Independent Integrals," Computational Methods in the Mechanics of Fracture, 1986, pp. 123-165.
7. Brust, F. W., McGowan, J. J., and Atluri, S. N., "A Combined Numerical-Experimental Study of Ductile Crack Growth after a Large Unloading, Using T*, J and CTOA Criteria," Engineering Fracture Mechanics, Vol. 23, 1986, pp. 537-550.
8. Wang, L., Brust, F. W., and Atluri, S. N., "The Elastic-Plastic Finite Element Alternating Method (EPFEAM) and the Predictions of Fracture Under WFD Conditions in Aircraft Structures, Part II: Fracture and the T*-Integral Parameter," FAA Center of Excellence for Computational Modeling of Aircraft Structures, Georgina Institute of Technology, 1995.
9. Kanninen, M. F., "The Analysis of Stable Crack Growth in Type 304 Stainless Steel," International Conference of Fracture, 1980, pp. 1759-1768.
10. Newman, J. C., Jr., "An Elastic-Plastic Finite Element Analysis of Crack Initiation, Stable Crack Growth, and Instability," ASTM STP 833, 1984, pp. 93-117.
11. Dawicke, D. S. and Newman, J. C., Jr., "Residual Strength Predictions for Multiple Site Damage Cracking Using a Three-Dimensional Finite Element Analysis and a CTOA Criterion," Submitted for Publication in Fatigue and Fracture Mechanics: 29th Volume, ASTM STP 1321, 1998.
12. Dawicke, D. S. and Newman, J. C., Jr., "Evaluation of Various Fracture Parameters for Predictions of Residual Strength in Sheets with Multi-Site Damage," Proccedings from the First Joint DoD/NASA/FAA Conference on Aging Aircraft, 1998.
13. Starnes, J. H., Jr., Rose, C. A., and Rankin, C. C., "Effects of Combined Loads on the Nonlinear Response and Residual Strength of Damaged Stiffened Shells," Proceedings of the FAA-NASA Symposium on the Continued Airworthiness of Aircraft Structures, 1996, pp. 183-196.
14. Koppenhoefer, K. C., Gullerud, A. S., Ruggieri, C. and Dodds, R. H., Jr., "WARP3D: Dynamic Nonlinear Analysis of Solids Using a Preconditioned Conjugate Gradient Software Architecture", Structural Research Series (SRS) 596, UILU-ENG-94-2017, University of Illinois at Urbana-Champaign, 1994.
15. Johnston, W. M. and Helm, J. D., "Experimental Results from the FAA/NASA Wide Panel Fracture Tests," Second Joint NASA/FAA/DoD Conference on Aging Aircraft, Williamsburg, VA, 1998..
16. Dawicke, D. S., "Residual Strength Predictions Using a CTOA Criterion," DOT/FAA/AR-97/2, Proceedings of the FAA-NASA Symposium on Continued Airworthiness of Aircraft Structures, July 1997, pp. 555-566.
17. Hughes, T. J., "Generalization of Selective Integration Procedures to Anisotropic and Nonlinear Media," International Journal for Numerical Methods in Engineering, Vol. 15, 1980, pp. 1413-1418.